2025, 10(44s) e-ISSN: 2468-4376

https://www.jisem-journal.com/

Research Article

Attention Tub: Harnessing Deep Attention Network for Tuberculosis Detection in Chest X-Rays

Shirley C P¹, Sai Diya R², Abinaya R³, S.Nagarajan^{4*}, Thanga Helina S⁵, Dr. G. Naveen Sundar⁶
¹Department of Computer Science and Engineering, Karunya Institute of Technology and Sciences, Coimbatore, India

shirleydavidlivingston@gmail.com

²Department of Computer Science and Engineering, Karunya Institute of Technology and Sciences, Coimbatore, India ³Department of Computer Science and Engineering, Karunya Institute of Technology and Sciences, Coimbatore, India ⁴Associate Professor, Division of Digital Sciences, Karunya Institute of Technology and Sciences, Coimbatore, Tamilnadu, India ⁵Department of Commerce with Computer Application, KPR College of Arts Science and Research, Coimbatore, India. ⁶Department of Computer Science and Engineering, Karunya Institute of Technology and Sciences, Coimbatore, India. naveensundar@karunya.edu

*Corresponding Author

ARTICLE INFO

ABSTRACT

Received: 30 Dec 2024 Revised: 12 Feb 2025 Accepted: 26 Feb 2025 Pulmonary tuberculosis (TB) is a significance issue for public health worldwide, thus requiring accurate and prompt diagnosis for effective prevention and treatment Chest x-ray (CXR) is an essential tool a for diagnosis due to its high cost and non-invasive nature. However, models for deep learning in particular convolutional neural networks (CNNs) often face challenges such as overfitting and difficulty in capturing subtle differences in lesion characteristics and in order to overcome that on these issues a new approach is proposed, the Deep Attention Network (DANet). The model adds layers for feature extraction, followed by maximal pooling procedures to reduce spatial dimensions. Skip connections facilitate gradient propagation during training, while external attention introduced through the connection layer enhances feature representation by focusing on appropriate image locations Global maximal pooling for feature collection its classification is simple, and results in binary classification tasks 99% accuracy. Remarkable accuracy in findings suggest that DANet can be a valuable tool to aid in clinical decision making, providing important support radiologists and medical professionals.

Keywords: Pulmonary Tuberculosis, Deep Learning, Convolutional Neural Networks (CNNs), Chest X-ray (CXR), Deep Attention Network (DANet), Feature Extraction, Clinical Decision Support

I. INTRODUCTION

Tuberculosis (TB) continues to be a serious global health concern, leading to millions of deaths annually worldwide. It impacts individuals of all ages, necessitating early identification for efficient care and better patient outcomes. Chest X-rays (CXRs) have become the principal technique for identifying pulmonary providing detailed views of lung structures to identify characteristic TB lesions. The depth of the networks significantly impacts the types of features extracted and utilized for classification. However, accurately classifying TB subtypes, such as drugsensitive and drug-resistant TB, is challenging due to subtle differences in lesion appearance. Manual interpretation of CXR images is subjective, time- intensive, and prone to errors, especially when dealing with a lot of cases. Consequently, there is growing interest in machine learning-based approaches for automated TB classification from CXR images, playing a crucial role in computer-aided diagnosis (CAD) systems.

In the study, improved (TB) classification algorithm using a collection of 7000 images has been proposed, including both normal cases and tuberculosis, with an impressive accuracy of 99%. Worldwide health concern, particularly in resource-limited areas where access to primary care is limited. Accurate and timely diagnosis for effective TB treatment and prevention, but traditional diagnostic methods often prove time-consuming The power of machine learning which the research suggests can greatly improve assessment accuracy while remaining scalable and affordable simple solutions To simplify, the work contributes to a growing body of research applying machine

2025, 10(44s) e-ISSN: 2468-4376

https://www.jisem-journal.com/

Research Article

learning to medical imaging, which determines TB diagnosis increasingly used in disease classification and healthcare delivery. The high accuracy achieved in TB classification system highlights its potential to transform TB diagnosis, facilitate early diagnosis and intervention, and ultimately contribute to global efforts to control the disease.

The study introduces an innovative approach to (TB) classification, which addresses important limitations of existing methods [1] and offers great potential to impact health care and extensive applications. The methodology, using o techniques such as oversampling and data enhancement of the TB dataset of 700 to 3500 samples, effectively scales the dataset and increases its diversity it delivers an impressive accuracy of 99 % and addresses the limitations of inbalanced datasets for reference [2]. The scalability and accessibility of system further sets it apart, providing a highly scalable solution that simplifies TB diagnosis, even in resource-limited settings.

The potential impact of research is substantial, facilitating the early diagnosis of TB with greater accuracy, accelerating the initiation of treatment, ultimately reducing disease transmission and improving treatment outcomes. Furthermore, our methods and analyses extend beyond tuberculosis classification, and are frequently employed in medical imaging and disease diagnosis. By demonstrating the versatility and relevance of work, we demonstrate its potential to impact health care and medical research areas. Looking ahead, system refinement, exploration of new imaging modalities, and clinical validation studies are key future directions to maximize the impact of our system in tuberculosis diagnosis and beyond.

The work contributes to further developments in neural network architecture design, focusing on image classification tasks. The proposed methods facilitate advanced feature extraction and segmentation by combining additional features such as residual blocks and combining them using the combined features from multiple transformation processes in residual blocks, the model enhances feature representation, encourages richer diverse representations of input images Techniques such as f- normalization are include improving model efficiency and preventing overfitting The choice of layout enables faster convergence during training and they make good use of computer resources. The remaining portion of the study is structured as follows: Section 2 provides background information and relevant literature, while Section 3 goes into greater detail on the suggested technique. Section 4 presents the results and dialogue are indicated, while the final section concludes the study.

II. BACKGROUND AND RELATED WORKS

Although the ResfEANet model [8] combines external attention mechanisms with ResNet, it has drawbacks but enhances feature extraction and attentional focus. Applications requiring real-time processing may be hindered by their growing complexity and high resource requirements. Moreover, reliance on outside attention could limit generalizability and adaptability, necessitating greater research for efficient application and optimisation in medical imaging and tuberculosis detection initiatives. Utilising T-SPOT and a CNN-based prediction model was the aim of the study, which was conducted at Tongji Hospital and Sino-French New City Hospital between January 2016 and January 2022 [10]. Up until the age of 19, distinguish between latent tuberculosis infection (LTBI) and active tuberculosis (ATB). Although it highlights the enhanced T-SPOT diagnostic value and the promise of artificial intelligence in illness detection, there are a number of important limitations, including the need for additional validation and difficulties with practical application. For precise segmentation and classification, the CAD method for detecting pulmonary tuberculosis [11] incorporates cutting-edge methods such dilated fusion blocks and attention mechanisms.

However, in environments with limited resources, its complexity and processing costs might prevent real-time deployment. Further research is required to determine the model's interpretability and generalizability to a variety of demographics, and thorough clinical validation is required in order to guarantee the model's dependability and obtain regulatory permission for clinical application. An Incremental Learning-based Cascaded (ILCM) model [12] that outperforms previously trained models is presented for the identification of TB cases found on chest x-ray However, Reliance on AI, however, could lead to 21higher processing needs and difficulties with model interpretability when it comes to filtering, disease categorization, and localization. Although image enhancement methods such as histogram calculation yield higher visibility by optimizing pixel values, more research is required to

2025, 10(44s) e-ISSN: 2468-4376

https://www.jisem-journal.com/

Research Article

ascertain how these methods affect diagnostic precision.

Furthermore, the cascaded technique introduces complexity, which may have an impact on robustness and scalability. To overcome these issues and guarantee the model's efficacy in clinical settings, more investigation is required. The model gives a thorough analysis of review of AI techniques for CXR imaging analysis [19], it may suffer from publication bias because of the exclusion and lack of non-English studies databases selected from therefore the requirement may introduce bias in selection, which could overlook valuable studies Limiting the inclusion of primary studies and excluding nonhuman studies and comparative studies exclusion can reduce the insights gained from studies

III. METHODOLOGY

The volume is a cornerstone of the study, offering thorough understanding of the systematic approach to investigate tuberculosis It describes the methods, techniques, and tools used to collect, analyze, and interpret data. A comprehensive view of a systematic approach to dealing with TB diagnosis has been adopted. It describes the methods. Techniques and tools we used to collect, analyze and interpret data. The main point, as shown for conventional networks such as "Dense-net", is that as the quantity of layers rises irrespective of the quantity of iterations, the training error increases because model the performance has decreased because of the saturation of accuracy achieved. To overcome the obstacle, the suggested model incorporates the addition of a new construction module. The block is built with carefully constructed convolutional layers and combination operations to enhance feature representation and capture complex patterns in data When integrated the introductory block into the model architecture, the aim to reconfigure learning processes is robust, allowing the model to get beyond the constraints imposed by accuracy saturation

1. Deep Attention Network

The identity block stands as a cornerstone within the model architecture, serving as a crucial element for enhancing feature representation. It is designed to meticulously refine the underlying characteristics of the input data, enabling model to capture intricate patterns effectively. Mathematically, the operations within the identity block can be expressed via a sequence of meticulously crafted transformations:

The identity block starts its refinement process by passing the data through a series of convolutional operations, represented as a, b, c, and d, given a feature map x with F filters. In order to extract hierarchical features of various levels of complexity, these convolutional layers function as complicated filters by carefully examining the spatial properties of the input feature map. The outputs of these convolutional layers are then processed using Rectified Linear Unit (ReLU) activations, which add non-linearity to the feature representation. This non-linearity is what allows the model to recognize different complex patterns and correlations in the input data. The intermediate feature maps generated by the convolutional layers and ReLU activations come in contact with each other.

The concatenation method increases the feature representation by considering a more comprehensive understanding of underlying data distribution and allows the model to capture both local information ([a, b]) as well as global [c][d]. Finally, after the concatenation a 1*1 convolutional layer is applied to concatenate feature maps. This is the convolutional layer that plays a very important role in both expanding the number of feature maps and improving ability to recognise complex patterns, correlations within data.

Additionally, a shortcut trigger is defined within the identity block to maintain significant data in the network. This residual connection technique is very useful in training because it lessens the vanishing gradient problem and therefore allows for more efficient flow of gradients during backpropagation which can help with steady convergence. Finally, the output feature maps are created as a summation of 1x1 convolutional layer result with the original input. WFLA just performs addition operation over the improved features obtained from previous processes, and combines them to give a global representation of X.

The identity block is an important piece to the model design that creates better feature representation. A quantitative layer, the operations of identity block is listed as follows for some step operation which aims to explain

2025, 10(44s) e-ISSN: 2468-4376

https://www.jisem-journal.com/

Research Article

what happens within for a better representation and the feature itself. Convolutional + ReLU layers Rectified Linear Unit (ReLU) activation is applied after series of convolutional operations (a, b, c and d on input feature map x). The identity block composed of three consecutive convolutional layers, each followed by a ReLU activation function. The measurements of the maps remain consistent over each block as there is a similar padding setup to 'same' for all convolutions. This is a common structure used in very deep convolutional networks where we want to increase the depth of our network while keeping spatial dimensions same.

Convolutional layers shown in eqn.1 helps to capture local as well global information in very efficient way;

Concatenate(
$$[a,b,c,d]$$
) = mid ----- 1

This implementation uses a one-dimensional 1x1 convolutional layer with an activation of the form ReLU activated 1x1 Convolution

Adding the 1x1 convolutional layer increases depth of concatenated feature maps and hence helps in learning by complex patterns. ReLU Activation ensures that the feature representation is non-linear as shown in eqn.2

To address this, a residual connection is added to maintain important information over the network and allow for easier gradient flow during training as shown in eqn.3.

$$x = \text{Conv2D}(x, 2F, 1) -----3$$

These feature maps is derived by summing up the output of 1x1 convolutional layer with input initial feature buffers as shown in eqn. 4.

$$y = Add([mid], x])$$
 ----- 4

Below, the calculater with resulting feature maps is subjected to another convolutional operation followed by ReLU activation as shown in eqn.5. In the subsequent line, it applies a second convolutional operation and activates each of this feature map with ReLU as shown in eqn.6.

$$y = \text{Conv2D}(x, 2F, 1) ----- 5$$

 $y = \text{ReLU}(y) ---- 6$

With mathematical expressions and theoretical approbations, this imbibes an in-depth account of the identity block introducing its equality into a deep learning model.

2025, 10(44s) e-ISSN: 2468-4376

https://www.jisem-journal.com/

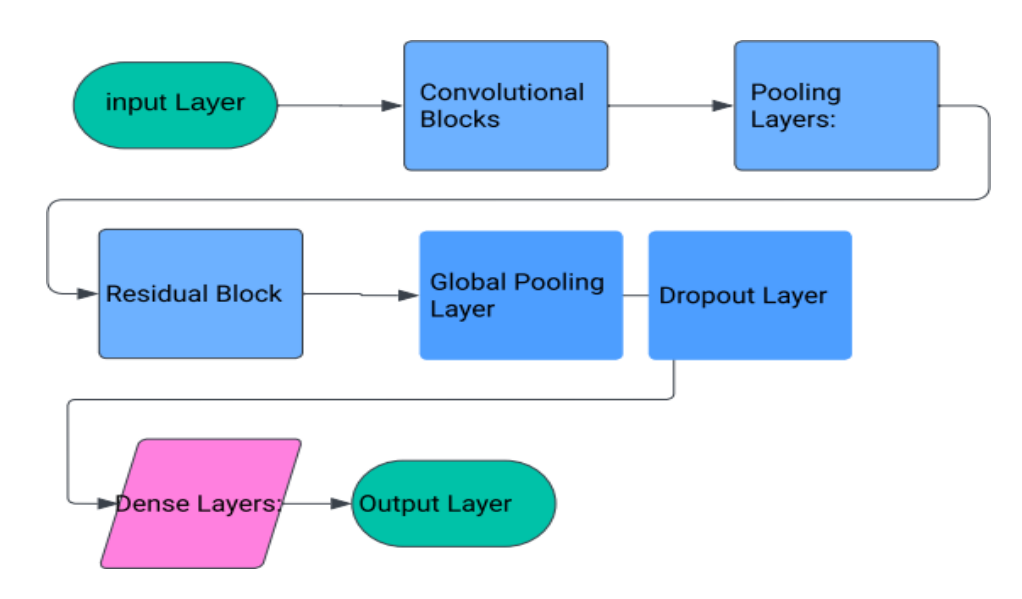


Fig 1. Methodology Overview

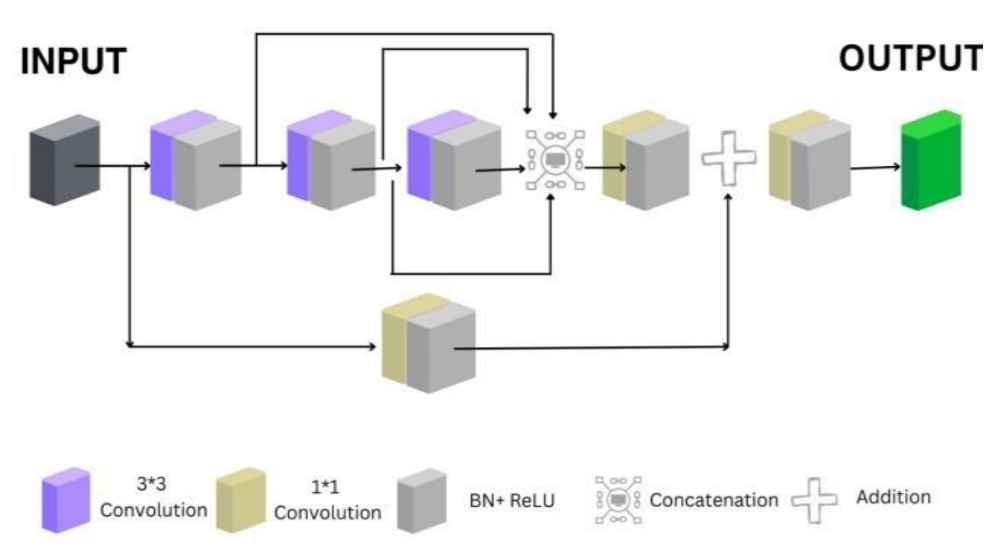


Fig 2. Model architecture

2025, 10(44s) e-ISSN: 2468-4376

https://www.jisem-journal.com/

Research Article

conv2d_59 (Conv2D)	(None, 15, 15, 256)	65792	['add_4[0][0]']
re_lu_34 (ReLU)	(None, 15, 15, 256)	0	['conv2d_59[0][0]']
<pre>global_max_pooling2d_4 (Gl obalMaxPooling2D)</pre>	(None, 256)	0	['re_lu_34[0][0]']
dropout_4 (Dropout)	(None, 256)	0	['global_max_pooling2d_4[0][0] ']
dense_12 (Dense)	(None, 128)	32896	['dropout_4[0][0]']
dense_13 (Dense)	(None, 64)	8256	['dense_12[0][0]']
dense_14 (Dense)	(None, 1)	65	['dense_13[0][0]']
Total manage 045035 (2.23 to			

Total params: 845825 (3.23 MB)

Trainable params: 845825 (3.23 MB) Non-trainable params: 0 (0.00 Byte)

Figure3.Model Summary

Flowchart of the model architecture is shown in Fig1 followed by 3D detailed model architecture demonstrated as shown in Fig2. Figure 3 provides a detailed Summary of the model.

Layer (type)	Output Shape	Param #	Connected to
input_5 (InputLayer)	[(None, 500, 500, 1)]	0	[]
conv2d_48 (Conv2D)	(None, 500, 500, 32)	320	['input_5[0][0]']
max_pooling2d_20 (MaxPooli ng2D)	(None, 250, 250, 32)	0	['conv2d_48[0][0]']
conv2d_49 (Conv2D)	(None, 250, 250, 32)	9248	['max_pooling2d_20[0][0]']
max_pooling2d_21 (MaxPooli ng2D)	(None, 125, 125, 32)	0	['conv2d_49[0][0]']
conv2d_50 (Conv2D)	(None, 125, 125, 32)	9248	['max_pooling2d_21[0][0]']
max_pooling2d_22 (MaxPooling2D)	(None, 62, 62, 32)	Ø	['conv2d_50[0][0]']
conv2d_51 (Conv2D)	(None, 62, 62, 64)	18496	['max_pooling2d_22[0][0]']
max_pooling2d_23 (MaxPooling2D)	(None, 31, 31, 64)	0	['conv2d_51[0][0]']
conv2d_52 (Conv2D)	(None, 31, 31, 64)	36928	['max_pooling2d_23[0][0]']

2025, 10(44s) e-ISSN: 2468-4376

https://www.jisem-journal.com/

Research Article

<pre>max_pooling2d_24 (MaxPooli ng2D)</pre>	(None, 15, 15, 64)	0	['conv2d_52[0][0]']
conv2d_53 (Conv2D)	(None, 15, 15, 128)	73856	['max_pooling2d_24[0][0]']
re_lu_28 (ReLU)	(None, 15, 15, 128)	0	['conv2d_53[0][0]']
conv2d_54 (Conv2D)	(None, 15, 15, 128)	147584	['re_lu_28[0][0]']
re_1u_29 (ReLU)	(None, 15, 15, 128)	0	['conv2d_54[0][0]']
conv2d_55 (Conv2D)	(None, 15, 15, 128)	147584	['re_lu_29[0][0]']
re_lu_30 (ReLU)	(None, 15, 15, 128)	0	['conv2d_55[0][0]']
conv2d_56 (Conv2D)	(None, 15, 15, 128)	147584	['re_lu_30[0][0]']
re_lu_31 (ReLU)	(None, 15, 15, 128)	0	['conv2d_56[0][0]']
<pre>concatenate_4 (Concatenate)</pre>	(None, 15, 15, 512)	0	['re_lu_28[0][0]', 're_lu_29[0][0]', 're_lu_30[0][0]', 're_lu_31[0][0]']
conv2d_57 (Conv2D)	(None, 15, 15, 256)	131328	['concatenate_4[0][0]']
conv2d_58 (Conv2D)	(None, 15, 15, 256)	16640	['max_pooling2d_24[0][0]']
re_1u_32 (ReLU)	(None, 15, 15, 256)	0	['conv2d_57[0][0]']
re_lu_33 (ReLU)	(None, 15, 15, 256)	0	['conv2d_58[0][0]']
add_4 (Add)	(None, 15, 15, 256)	0	['re_lu_32[0][0]', 're_lu_32[0][0]']

Fig 5. Sample Dataset

2. The Dataset:

The dataset shown in Fig 5 for the experiment is taken from Kaggle. In the systematic approach we have undertaken to handle the detection of tuberculosis. It outlines the strategies, techniques, and tools we have employed to collect, analyze, and interpret data. Identification of different illness states in It has been demonstrated that the human body is dependable when using X-ray and/or CT images from different areas of the body. Medical imaging of the chest in the form of X-rays, is used for the identification and management of tuberculosis, since the disease states are known to result from abnormalities experienced in the chest region.

In the research paper, discussing the dataset is essential as it provides crucial context regarding information utilized for validation, testing, and training. This data aids readers in comprehending the study's scope., the characteristics of the dataset, and the relevance of the findings. Here's a theoretical explanation to include in research paper. The dataset utilized in this study is essential to the creation and assessment of the suggested model. for tuberculosis detection using medical imaging. It comprises a collection of grayscale chest X-ray images obtained from diverse sources, including medical repositories and clinical settings.

Training Set: It consists of a large number of chest X-ray images meticulously curated to facilitate the training. The images are divided into two distinct classes: "NORMAL" and "TUBERCULOSIS", representing the absence and presence of tuberculosis, respectively. The training set contains total images of 4900 containing normal and tuberculosis class. Each image in the training set is resized to a standardized dimension of (img height times img width) of (500,500) pixels to ensure uniformity across the dataset.

2025, 10(44s) e-ISSN: 2468-4376

https://www.jisem-journal.com/

Research Article

Testing Set: Similarly, the testing set encompasses a separate set of chest X-ray images, distinct from those used in training. These images are reserved exclusively for measuring the performance of the trained model on unseen data. The testing set contains total images of 700 containing normal and tuberculosis class. Like the training set, the testing set contains images categorized into the "NORMAL" and "TUBERCULOSIS" classes.

Validation Set: Aiding in the fine-tuning of model hyperparameters and monitoring its generalization performance. The training, testing and validation subsets of order in ratio of (70,10,20) percent of total data to assess the model's performance. The methodology ensured the results' dependability and generalizability by enabling extensive validation across various combinations of training, validation sets. comprises chest X-ray images of 1400 containing normal and tuberculosis class. allowing for robust validation of the model's performance.

Data Augmentation: To enhance the training data and improve the model's ability to generalize, data augmentation techniques such as rotation, scaling, and horizontal flipping may be applied. These techniques introduce variations of training images, simulating real-world scenarios and preventing overfitting.

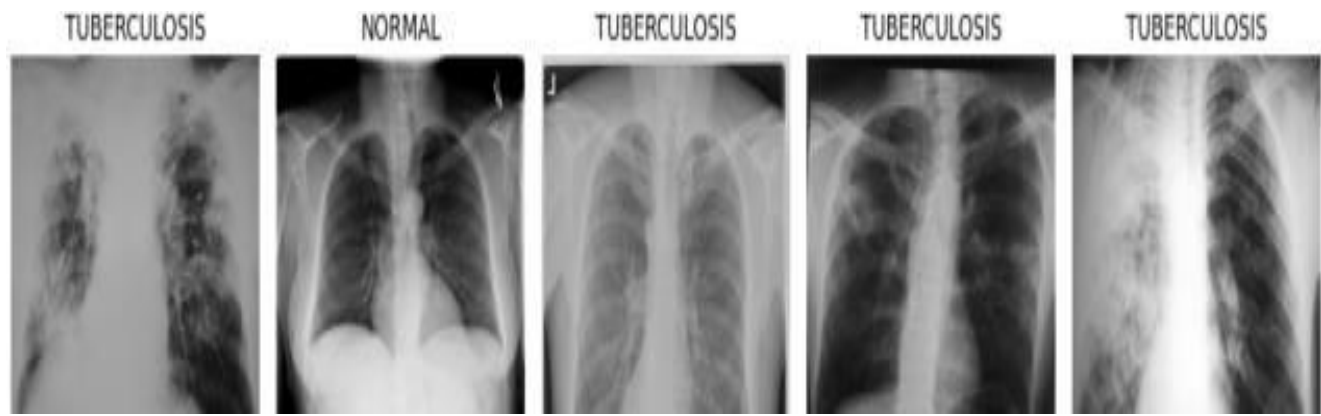


Fig 6. Chest X-RAY images

In the Fig.6 presented, a subset of images from the training set is visualized to provide a glimpse into the dataset's composition. Every image has a class name ("TUBERCULOSIS" or "NORMAL") next to it, making it easier to examine and understand the features of the collection visually. format guarantee uniformity and dependability during the trial procedure, which eventually adds to the validity and

IV. Experimental Environment Setup Hardware:

The computer system used in the study's experimental technique has specific hardware configurations that were optimised for deep neural network training. The hardware included an Intel(R) (TM) i5 CPU with 8GB of RAM and a GPU with an interface. The CNN architecture was built using Python programming, the TensorFlow and Keras frameworks, and other necessary components.. Instead of using pre-trained models, the decision was made to train the model from scratch because this enables a more thorough and dataset's photos and offers information about how the "NORMAL" and "TUBERCULOSIS" instances are distributed in terms of class. Understanding the dataset's characteristics.

V. Results and Discussion

This section contains the presentation and analysis of the results from the methodical application of our approach. We examine the statistics, graphs, and figures that best represent the findings of our investigation and offer a thorough analysis of the patterns, trends, and connections that the findings have uncovered. Following an experiment, it is normal to assess the results in order to compare the results with other models and determine whether the results can be applied in the future. The metrics we are using to assess the model and our

2025, 10(44s) e-ISSN: 2468-4376

https://www.jisem-journal.com/

Research Article

```
methodology are sensitivity, specificity, and accuracy.
TP + TN
     Accuracy =
TP + TN + FP + FN
  TP
           Precision =
     TP + FP
          TP
            Recall =
          TP + FN
                  2 * precison * recall
      F1 score =
precision + recall
```

	precision	recall	f1-score	support
NORMAL TUBERCULOSIS	1.00 1.00	1.00 1.00	1.00 1.00	350 350
accuracy macro avg weighted avg	1.00 1.00	1.00 1.00	1.00 1.00 1.00	700 700 700

Fig 7. Experimental results

Following 10 epochs of 307 batches, for which the training was halted using an early stopping set at 10 epochs, the outcome of the training is displayed in Table 1 below, Fig 7. Above displays the depiction of the validation and training accuracy. The model stopped early since it showed improvement in accuracy despite the training accuracy increasing gradually from 92% to 99%. The accuracy of the training increased to 99%. Following the subsequent 70% of training, a comparatively sluggish convergence progression with the accuracy reaching with 94% accuracy at 50% of the training epoch and 97% accuracy after 75%. The training loss continued to decline after that, going from roughly 34% to roughly 0.4%. Table 2 displays the comparison results of several model. Figure 8 below displays the confusion matrix derived. The camparision has been done for the experimental results before and after balancing the data set. The model Accuracy has varied from 97% to 99% by balancing the datset of (TB). The confusion matrix and the plot for the accuracy and loss has been studied and given below.

2025, 10(44s) e-ISSN: 2468-4376

https://www.jisem-journal.com/

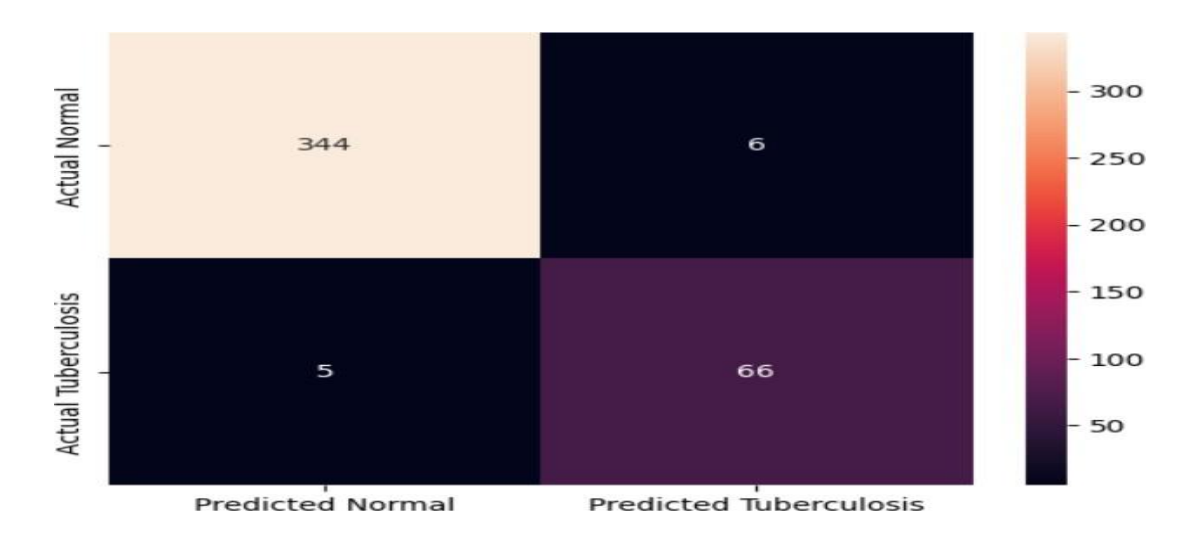


Fig 8. Confusion Matrix before balancing dataset

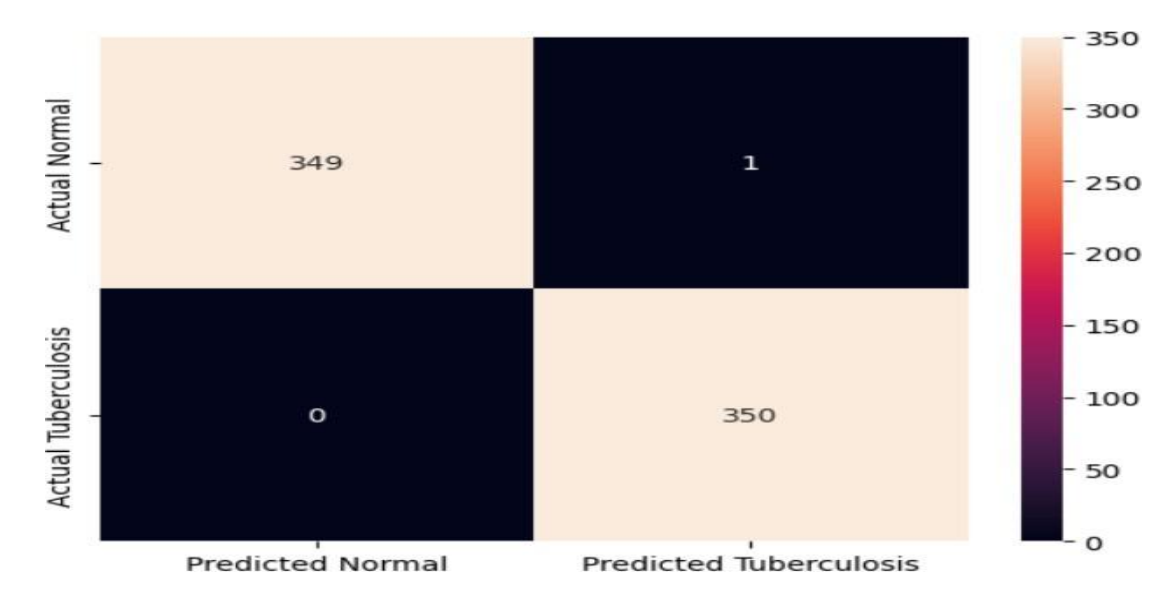


Fig 9. Confusion Matrix after balancing dataset

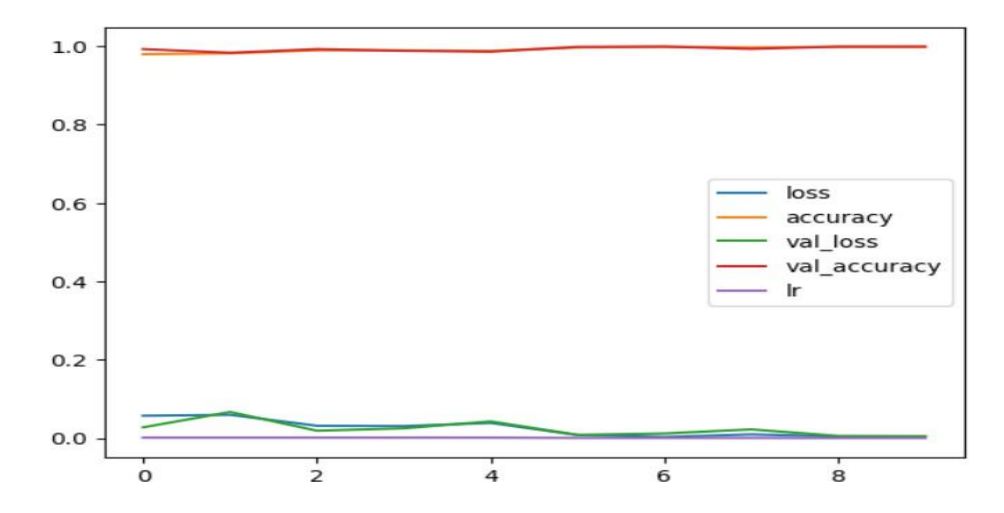


Fig 10. Plot of Accuracy and Loss before balancing

2025, 10(44s) e-ISSN: 2468-4376

https://www.jisem-journal.com/

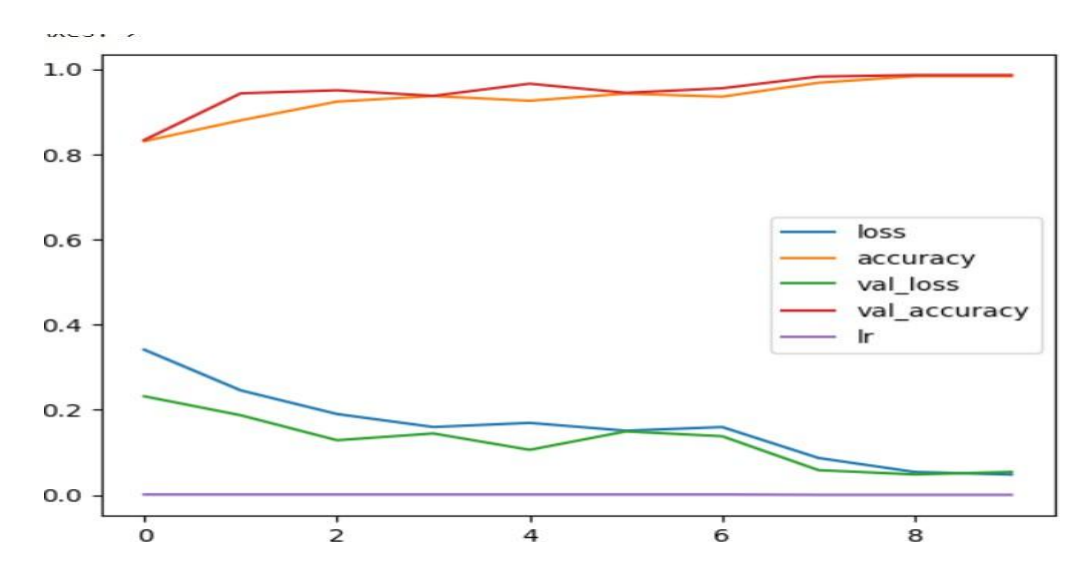


Fig 11. Plot of Accuracy and loss After balancing

100.00% probability of being Normal case Actual case : NORMAL



Fig 12. Classification Image1

98.57% probability of being Normal case Actual case : NORMAL

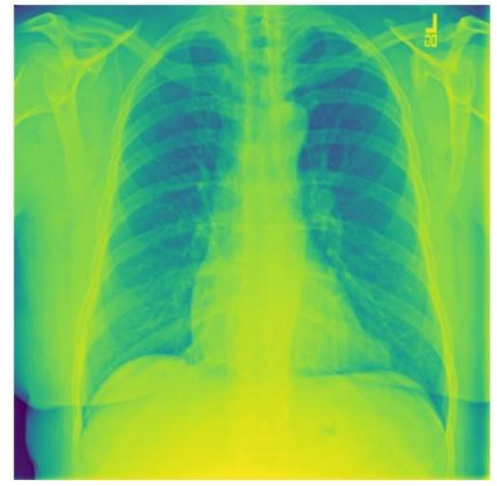


Fig 13. Classification Image2

MODEL	Accuracy	Precison	
Densenet 169	95.2	94.4	
Hybrid segmentation	96.0	95.0	
VGG16	95.4	93.4	
sCNN	93.3	90.0	
RenseNet50	97.83	97.67	
Densenet 201	94.9	91.4	
DANet(proposed)	99.0	100	

Table 1. Experimental results of different model

2025, 10(44s) e-ISSN: 2468-4376

https://www.jisem-journal.com/

Research Article

VI. Conclusion

TB requires early and precise diagnosis for efficient treatment and prevention. The chest x-ray (CXR), because of its simple nature and high expense, is an important diagnostic tool. frequently encounter problems like overfitting and have trouble identifying minute variations in lesion features. To address these problems, a novel strategy called the Deep Attention Network is put forth. DANet. In order to extract features, DANet incorporates convolutional layers. To minimize spatial dimensions, maximal pooling procedures are then applied. While external attention introduced through the connection layer improves feature representation by focusing on appropriate image areas, skip connection helps gradient propagation during training. Its categorization is simple because of global maximum pooling and dense layer feature pooling, and the dense layers to gather features Its straightforward classification yields 99% accuracy in binary classification problems. Remarkable accuracy in results indicates that DANet is a useful tool to support radiologists and other medical professionals in their clinical decision- making.

REFERENCES

- [1] A. R. Laeli, Z. Rustam and J. Pandelaki, "Tuberculosis Detection based on Chest X-Rays using Ensemble Method with CNN Feature Extraction," 2021 International Conference on Decision Aid Sciences and Application (DASA), Sakheer, Bahrain, 2021, pp. 682-686, doi: 10.1109/DASA53625.2021.9682237
- [2] Alebiosu, D. O., Dharmaratne, A., & Lim, C. H. (2023). Improving tuberculosis severity assessment in computed tomography images using novel DAvoU-Net segmentation and deep learning framework. *Expert Systems with Applications*, 213, 119287.
- [3] B. Oltu, S. Güney, B. Dengiz and M. Ağıldere, "Automated Tuberculosis Detection Using Pre-Trained CNN and SVM," 2021 44th International Conference on Telecommunications and Signal Processing (TSP), Brno, Czech Republic, 2021, pp. 92-95, doi: 10.1109/TSP52935.2021.9522644.
- [4] Bhandari, M., Shahi, T. B., Siku, B., & Neupane, A. (2022). Explanatory classification of CXR images into COVID-19, Pneumonia and Tuberculosis using deep learning and XAI. *Computers in Biology and Medicine*, 150, 106156.
- [5] Bhattacharyya, A., Bhaik, D., Kumar, S., Thakur, P., Sharma, R., & Pachori, R. B. (2022). A deeplearning based approach for automatic detection of COVID-19 cases using chest X-ray images. *Biomedical Signal Processing and Control*, 71, 103182.
- [6] Chandra, T. B., Singh, B. K., & Jain, D. (2022). Disease localization and severity assessment in chest X-ray images using multi-stage superpixels classification. *Computer Methods and Programs in Biomedicine*, 222, 106947.
- [7] Das, P. K., Sreevatsav, S., & Abraham, A. (2024). An efficient deep learning network with orthogonal softmax layer for automatic detection of tuberculosis. *Engineering Applications of Artificial Intelligence*, 133, 108116.
- [8] Ejiyi, C. J., Qin, Z., Nnani, A. O.,
- [9] Deng, F., Ejiyi, T. U., Ejiyi, M. B., ... & Bamisile, O. (2024). ResfEANet: ResNet-fused external attention network for tuberculosis diagnosis using chest X-ray images. *Computer Methods and Programs in Biomedicine Update*, 5, 100133.
- [10] Hasan, M. M., Hossain, M. M.,
- [11] Rahman, M. M., Azad, A. K. M., Alyami, S. A., & Moni, M. A. (2023). FP-CNN: Fuzzy pooling-based convolutional neural network for lung ultrasound image classification with explainable AI. *Computers in Biology and Medicine*, 165, 107407.
- [12] Huang, M. L., & Liao, Y. C. (2022). A lightweight CNN-based network on COVID-19 detection using X-ray and CT images. *Computers in Biology and Medicine*, *146*, 105604.
- [13] Iqbal, A., Sharif, M., Khan, M. A., Nisar, W., & Alhaisoni, M. (2022). FF-UNet: a U- shaped deep convolutional neural network for multimodal biomedical image segmentation. *Cognitive Computation*, 14(4), 1287-1302.
- [14] Iqbal, A., Usman, M., & Ahmed, Z. (2023). Tuberculosis chest X-ray detection using CNN-based hybrid segmentation and classification approach. Biomedical Signal Processing and Control, 84, 104667.
- [15] Ismael, A. M., & Şengür, A. (2021). Deep learning approaches for COVID-19 detection based on chest X-ray images. *Expert Systems with Applications*, *164*, 114054.
- [16] Liang, S., Ma, J., Wang, G., Shao, J., Li, J., Deng, H., ... & Li, W. (2022). The application of artificial

2025, 10(44s) e-ISSN: 2468-4376

https://www.jisem-journal.com/

- intelligence in the diagnosis and drug resistance prediction of pulmonary tuberculosis. *Frontiers in medicine*, *9*, 935080.
- [17] Luo, Y., Xue, Y., Liu, W., Song, H., Huang, Y., Tang, G., ... & Sun, Z. (2023).
- [18] Convolutional neural network based on T-SPOT. TB assay promoting the discrimination between active tuberculosis and latent tuberculosis infection. *Diagnostic Microbiology and Infectious Disease*, 105(3), 115892.
- [19] Momeny, M., Neshat, A. A., Gholizadeh, A., Jafarnezhad, A., Rahmanzadeh, E., Marhamati, M., ... & Zhang, Y. D. (2022). Greedy Autoaugment for classification of mycobacterium tuberculosis image via generalized deep CNN using mixed pooling based on minimum square rough entropy. Computers in Biology and Medicine, 141, 105175.[2]
- [20] Namuganga, A. R., Nsereko, M., Bagaya, B. S., Mayanja-Kizza, H., & Chegou, N. N. (2023). Differential expression of host protein biomarkers among symptomatic clinic attendees finally diagnosed with tuberculosis and other respiratory diseases with or without latent Mycobacterium tuberculosis infection. *Immunology Letters*, 253, 8-
- [21] Richards, A. S., Sossen, B., Emery, J. C., Horton, K. C., Heinsohn, T., Frascella, B., ... & Houben, R. M. (2023). Quantifying progression and regression across the spectrum of pulmonary tuberculosis: a data synthesis study. *The Lancet Global Health*, 11(5), e684-e692.
- [22] Sajed, S., Sanati, A., Garcia, J. E., Rostami, H., Keshavarz, A., & Teixeira, A. (2023). The effectiveness of deep learning vs. traditional methods for lung disease diagnosis using chest X-ray images: A systematic review. *Applied Soft Computing*, 110817.
- [23] Savage, H. R., Rickman, H. M., Burke, R. M., Odland, M. L., Savio, M., Ringwald, B., ... & MacPherson, P. (2023). Accuracy of upper respiratory tract samples to diagnose Mycobacterium tuberculosis: a systematic review and meta-analysis. *The Lancet Microbe*.
- [24] Sossen, B., Richards, A. S., Heinsohn, T., Frascella, B., Balzarini, F., Oradini- Alacreu, A., ... & Esmail, H. (2023). The natural history of untreated pulmonary tuberculosis in adults: a systematic review and meta-analysis. *The Lancet Respiratory Medicine*.
- [25] Tan, Z., Madzin, H., Norafida, B.,
- [26] ChongShuang, Y., Sun, W., Nie, T., & Cai, F. (2024). DeepPulmoTB: A benchmark dataset for multi-task learning of tuberculosis lesions in lung computerized tomography (CT). *Heliyon*.
- [27] Vats, S., Sharma, V., Singh, K., Katti, A., Ariffin, M. M., Ahmad, M. N., ... & Salahshour, S. (2024). Incremental learning-based cascaded model for detection and localization of tuberculosis from chest x-ray images. *Expert Systems with Applications*, 238, 122129.